

Title No. 113-S25

Analysis of Steel Fiber-Reinforced Concrete Elements Subjected to Shear

by Seong-Cheol Lee, Jae-Yeol Cho, and Frank J. Vecchio

In this paper, a rational analysis procedure is presented for modeling the shear behavior of steel fiber-reinforced concrete (SFRC) elements. In the development of the analysis procedure, the Disturbed Stress Field Model (DSFM), based on the Modified Compression Field Theory (MCFT), is modified by implementing constitutive models for SFRC, which are derived from the Diverse Embedment Model (DEM). For the contribution of steel fibers, a local stiffness matrix for fibers has been developed separately from those for concrete matrix and conventional reinforcement. The composite element stiffness matrix for an SFRC element with conventional reinforcement is then derived by superposing the three local stiffness matrixes. In the element stiffness matrix, the effect of shear slip at a crack is also taken into account by considering the resistance due to steel fibers against shear stress on crack surface. Through comparisons with the test results of SFRC panels previously reported in the literature, it is shown that the actual shear behavior of SFRC panels are accurately predicted by the proposed analysis procedure, not only for the shear strength but also for the shear strain at the failure. Through implementation into finite element analysis programs, the analysis procedure developed in this paper can be useful in the modeling of SFRC members and structures also containing conventional reinforcement.

Keywords: finite elements; shear strain; shear strength; steel fiber; steel fiber-reinforced concrete (SFRC).

INTRODUCTION

It is well known that steel fiber-reinforced concrete (SFRC) exhibits ductile tensile behavior even after cracking because of the pullout behavior of steel fibers bridging the cracks. For the past several decades, much research has been conducted to evaluate the tensile behavior of SFRC through experimental programs¹⁻⁵ or analytical model developments.⁵⁻¹⁰ In CEB-FIP Model Code 2010,¹¹ as the result of these investigations, the tensile resistance of SFRC is included in the design of concrete structures; the tensile stress of SFRC can be evaluated from the results of four-point bending tests on notched beams in accordance with BS EN 14561.¹² Several researchers focused on whether steel fibers can be used to replace shear reinforcement in a reinforced concrete beam; Dinh et al.¹³ measured the ultimate shear strength of SFRC beams with conventional reinforcement while Susetyo et al.¹⁴ experimentally investigated the shear behavior of SFRC panels with conventional reinforcement. ACI 318-11¹⁵ conditionally allows the use of steel fibers of 0.75% in volume as minimum shear reinforcement in reinforced concrete beams.

Although remarkable progress has been made in SFRC research, as described previously, SFRC is not yet widely used in structural applications because it is still difficult to theoretically predict the structural behavior of SFRC

members with conventional reinforcement. Evidence of this was given by Susetyo et al.,¹⁶ who analyzed the SFRC panels they tested by implementing the Variable Engagement Model (VEM)⁷ and direct tension test results within a nonlinear finite element analysis method based on the Disturbed Stress Field Model (DSFM).^{17,18} They found that the analysis results were significantly affected by the selection of tension stiffening/softening models, shear slip on crack surfaces, and crack spacing parameters. This indicates the necessity to develop a more rational analysis procedure to predict the structural behavior of SFRC members with conventional reinforcement, especially in regards to the shear behavior, as many research efforts^{13,14,16} have focused on SFRC to partially or entirely replace the shear reinforcement in concrete members.

In this paper, therefore, an advanced analysis procedure for the shear behavior of SFRC panels with conventional reinforcement is presented. For the development of the analysis procedure, stresses and strains in the panels are explored in depth through a theoretical approach, and then recently developed models based on the Diverse Embedment Model (DEM)^{8,9} are employed to evaluate the structural behavior of SFRC with or without conventional reinforcement.

RESEARCH SIGNIFICANCE

Recently, several constitutive models,^{8-10,19} based on the DEM, were developed to represent the structural behavior of SFRC with or without conventional reinforcement. Although the uniaxial behavior of SFRC members can be modeled reasonably well with them, the shear behavior of SFRC members was not rationally captured.

The analysis procedure developed in this paper makes it possible to predict not only the uniaxial behavior but also the shear behavior of SFRC members with conventional reinforcement. The procedure described can be easily implemented in both an existing sectional analysis program²⁰ and finite element analysis programs²¹: each layer or each element can be modeled as a reinforced concrete element subjected to biaxial stress conditions and then it can be analyzed by employing the developed analysis procedure. Thus, the analysis procedure described will be useful in modeling the structural behavior of SFRC members and structures with conventional reinforcement.

ACI Structural Journal, V. 113, No. 2, March-April 2016.

MS No. S-2014-362.R1, doi: 10.14359/51688474, was received June 12, 2015, and reviewed under Institute publication policies. Copyright © 2016, American Concrete Institute. All rights reserved, including the making of copies unless permission is obtained from the copyright proprietors. Pertinent discussion including author's closure, if any, will be published ten months from this journal's date if the discussion is received within four months of the paper's print publication.

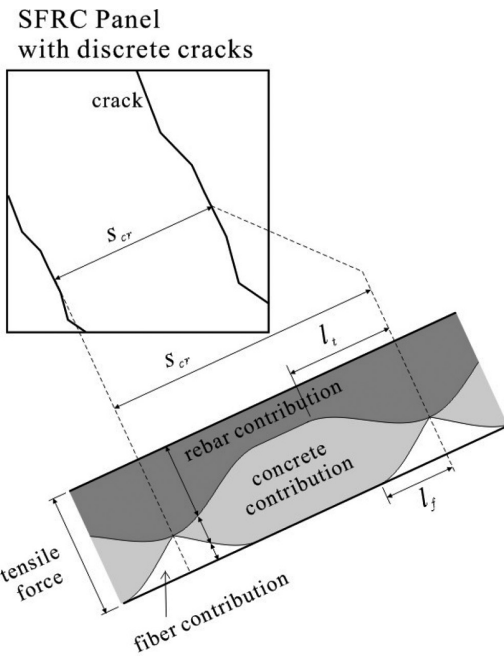


Fig. 1—Local tensile stress distribution in SFRC element.

STRESSES AND STRAINS IN SFRC PLANAR ELEMENTS

Stresses in SFRC element

To analyze the shear behavior of an SFRC planar element, one must evaluate the stresses in three materials: namely, the concrete matrix, conventional deformed reinforcing bar, and steel fibers. Figure 1 shows the stress distribution in each material in the principal tensile direction. As illustrated in the figure, with no consideration given to tension softening effects, the stress in the concrete matrix is zero at a crack, while the stresses in the other two materials are highest at a crack. Between the cracks, because tensile stresses are shared by the concrete matrix due to the bond mechanism between concrete matrix and the other two materials, the stress contributions from the three materials vary along the principal tensile direction. For simplicity of calculations, and as already adopted and verified in the DSFM and the MCFT,²² use of the “average stresses” concept, rather than a rigorous consideration of stress variation, was expected to work well. Therefore, the stresses in a SFRC element were idealized by employing a smeared crack model, as illustrated in Fig. 2.

For the tensile stresses resisted by the concrete matrix and conventional reinforcement, the average stresses can be obtained from tension-stiffening and tension-softening models and bilinear or trilinear models, respectively. On the other hand, the tensile stress in steel fibers at a crack can be evaluated from the DEM or the simplified DEM (SDEM).¹⁰ In this paper, therefore, the coefficient α_{avg} has been introduced to relate the tensile stress in steel fibers at a crack with the average tensile stress. Details will be presented in the discussion of constitutive relations that follow.

In addition to the average stresses, the shear stress and slip on crack surfaces should be considered because they could be significant factors influencing the shear behavior of SFRC panels subjected to shear. As presented in Fig. 3, the shear

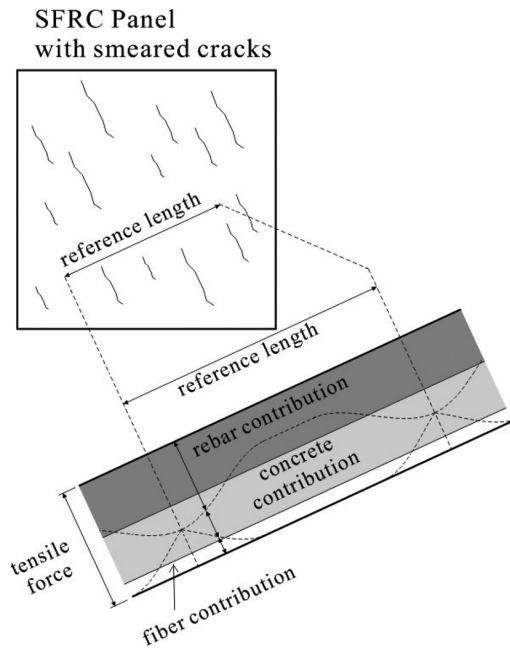


Fig. 2—Average tensile stresses in SFRC element with smeared crack.

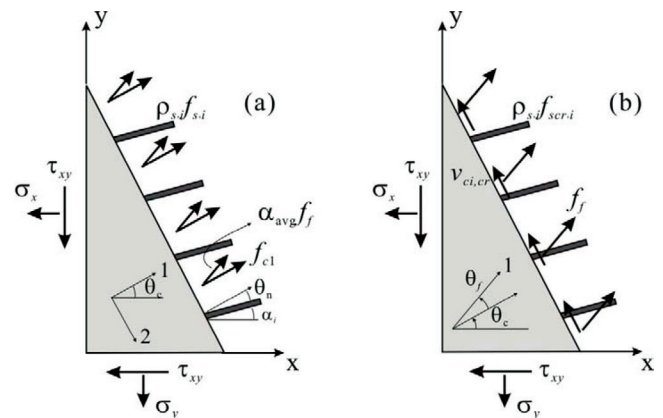


Fig. 3—Average and local stresses in SFRC element: (a) average stresses; and (b) local stresses.

stress on a crack surface can be evaluated through a comparison between the average stresses under smeared crack status and the local stresses at a crack, as in the following equation

$$v_{ci,cr} = \sum_i \rho_{s,i} (f_{scr,i} - f_{s,i}) \sin \theta_{n,i} \cos \theta_{n,i} - (1 - \alpha_{avg}) f_f \sin \theta_f \quad (1)$$

where $v_{ci,cr}$ is the shear stress on crack surface that is resisted by the concrete matrix, including aggregate interlock.

In Eq. (1), the term $(1 - \alpha_{avg}) f_f \sin \theta_f$ represents the contribution of steel fibers bridging a crack. Without steel fibers, the equation converges to the equation for normal reinforced concrete panel as presented in the DSFM. From the shear stress on the crack surface, shear slip on the crack surface can be calculated from the conventional model discussed in the “Constitutive relations” section that follows.

Strains in SFRC element

In the DSFM formulation, total strains and net strains are separately defined considering the effect of slip; the

total strains are the apparent (measured) strains that include deformations due to slip at a crack, while the net strains are concrete strains deduced from the apparent strains by subtracting the strains due to the shear slip at a crack, as illustrated in Fig. 4.

The strains due to the shear slip at a crack are calculated as

$$[\epsilon^s] = \begin{bmatrix} \epsilon_x^s \\ \epsilon_y^s \\ \gamma_{xy}^s \end{bmatrix} = \begin{bmatrix} -(\gamma_s/2) \sin(2\theta_c) \\ (\gamma_s/2) \sin(2\theta_c) \\ \gamma_s \cos(2\theta_c) \end{bmatrix} \quad (2)$$

where $\gamma_s = \delta_s/s_{cr}$ is an average shear slip strain; and θ_c is an inclination of principal net tensile strain in concrete.

Hence, the relationship between the total strains, $[\epsilon]$, and the net strains, $[\epsilon_c]$, are as follows

$$[\epsilon] = [\epsilon_c] + [\epsilon^s] \quad (3)$$

where $[\epsilon] = [\epsilon_x \ \epsilon_y \ \gamma_{xy}]^T$; and $[\epsilon_c] = [\epsilon_{cx} \ \epsilon_{cy} \ \gamma_{cxy}]^T$.

For the evaluation of stresses within the three materials (concrete matrix, steel fibers, and conventional reinforcement) in a SFRC planar element, the total strains are compatible with the constitutive law for conventional reinforcement while the net strains are compatible with the constitutive laws for concrete matrix and steel fibers.

CONSTITUTIVE RELATIONS

Models for SFRC without conventional reinforcement

SFRC can exhibit a ductile compressive behavior after peak stress that is quite different from that of normal concrete because the steel fibers mitigate against post-peak splitting cracks. In addition, the strain at the peak stress of SFRC is generally greater than that of normal concrete.²³ To reflect the effect of steel fibers on the compressive behavior, the model proposed by Lee et al.²³ has been adopted, which had been developed from the test results of 48 cylinder specimens with 150 mm (6 in.) diameter and 300 mm (12 in.) height.

$$f_{c2} = f_{c2max} \left[\frac{A(\epsilon_{c2}/\epsilon'_c)}{A-1 + (\epsilon_{c2}/\epsilon'_c)^B} \right] \quad (4)$$

where $A = B = 1/[1 - (f'_c/\epsilon'_c E_c)]$ for the pre-peak ascending branch, and $A = 1 + 0.723(V_f l_f/d_f)^{-0.957}$, $B = (f'_c/50)^{0.064}[1 + 0.882(V_f l_f/d_f)^{-0.882}] \geq A$ for the post-peak descending branch, and f_{c2max} is the maximum compressive stress considering the compression softening effect, as follows²¹

$$\frac{f_{c2max}}{f'_c} = \frac{1}{1 + 0.19(-\epsilon_{c1}/\epsilon_{c2} - 0.28)^{0.8}} \quad (5)$$

where $-\epsilon_{c1}/\epsilon_{c2} > 0.28$.

The elastic modulus of SFRC and the strain at the compressive strength, if not known, can be estimated from Eq. (6) and (7)²³

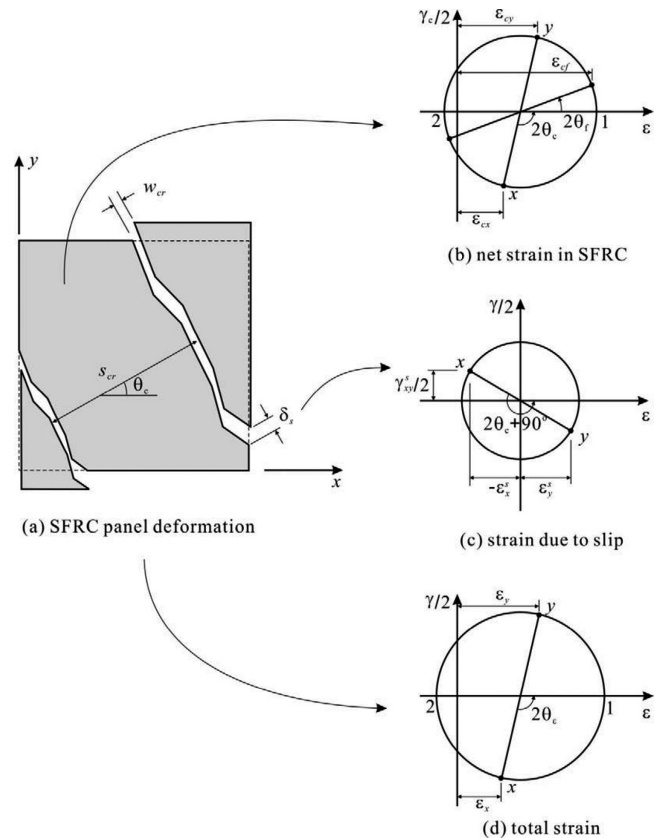


Fig. 4—Strains in SFRC element: (a) SFRC element deformation; (b) net strain for SFRC; (c) strain due to slip; and (d) total strain.

$$E_c = \left(-367V_f \frac{l_f}{d_f} + 5520 \right) f'_c{}^{0.41} \quad (6)$$

$$\epsilon'_c = \left(0.0003V_f \frac{l_f}{d_f} + 0.0018 \right) f'_c{}^{0.12} \quad (7)$$

To represent the tensile behavior of SFRC which exhibits ductile behavior even after cracking, the formulations of the DEM^{8,9} and the SDEM¹⁰ have been adopted. In the DEM, the tensile stress at a crack due to steel fibers can be rigorously calculated for a given crack width, through a double numerical integration scheme, to evaluate the average fiber tensile stress at a crack as follows

$$f_f = \alpha_f V_f \sigma_{f,cr,avg} \quad (8)$$

where $\sigma_{f,cr,avg} = \frac{2}{l_f} \int_0^{l_f/2} \int_0^{\pi/2} \sigma_{f,cr}(l_a, \theta) \sin \theta d\theta dl_a$.

Because the double numerical integration makes the calculation quite demanding, the DEM was simplified to the SDEM in which the bond mechanism for the pullout behavior of steel fibers and mechanical anchorage effect due to end-hooks are separately evaluated, as follows

$$f_f = f_{st} + f_{eh} \quad (9)$$

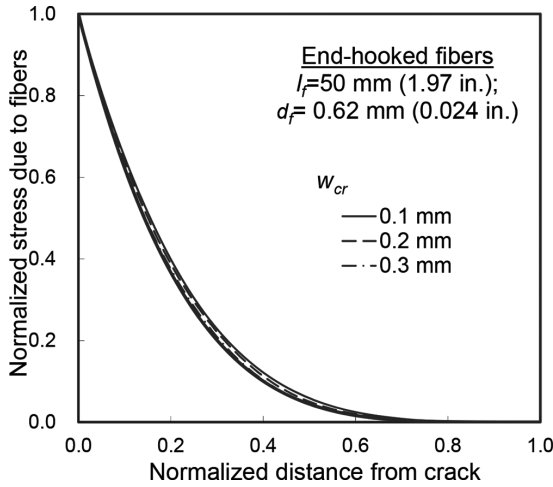


Fig. 5—Distribution of tensile stress in steel fibers at distance from a crack. (Note: 1 mm = 0.0394 in.)

$$f_{st} = \alpha_f V_f K_{st} \tau_{f,max} \frac{l_f}{d_f} \left(1 - \frac{2w_{cr}}{l_f}\right)^2 \quad (10)$$

$$f_{eh} = \alpha_f V_f K_{eh} \tau_{eh,max} \frac{2(l_i - 2w_{cr})}{d_f} \quad (11)$$

where

$$K_{st} = \begin{cases} \frac{\beta_f w_{cr}}{3 s_f} & \text{for } w_{cr} < s_f \\ 1 - \sqrt{\frac{s_f}{w_{cr}}} + \frac{\beta_f}{3} \sqrt{\frac{s_f}{w_{cr}}} & \text{for } w_{cr} \geq s_f \end{cases} \quad (12)$$

$$K_{eh} = \begin{cases} \beta_{eh} \left[\frac{2w_{cr}}{3s_{eh}} - \frac{1}{5} \left(\frac{w_{cr}}{s_{eh}} \right)^2 \right] & \text{for } w_{cr} < s_{eh} \\ 1 + \left(\frac{7\beta_{eh}}{15} - 1 \right) \sqrt{\frac{s_{eh}}{w_{cr}}} - \frac{2(\sqrt{w_{cr}} - \sqrt{s_{eh}})^2}{l_f - l_i} & \text{for } s_{eh} \leq w_{cr} < \frac{l_f - l_i}{2} \\ \left(\frac{l_i - 2w_{cr}}{2l_i - l_f} \right)^2 K_{eh,i} & \text{for } \frac{l_f - l_i}{2} \leq w_{cr} < \frac{l_i}{2} \end{cases} \quad (13)$$

It should be noted that the SDEM is applicable in most cases but only the DEM is suitable for SFRC in which fiber rupture is expected; fiber rupture is not considered in the SDEM.

As illustrated in Fig. 1, the tensile stress due to steel fibers varies between cracks, so the average for the tensile stress due to steel fibers through cracks should be evaluated. Employing the DEM, it is possible to evaluate the magnitude of the tensile stress transmitted from the steel fibers to the concrete matrix between cracks, as illustrated in Fig. 5. Based on the results of the DEM, a simple model for the coefficient α_{avg} over the average crack spacing has been derived as

$$\alpha_{avg} = \frac{2}{5.5} \frac{l_f}{s_{cr}} \leq 1.0 \quad (14)$$

It should be noted that Eq. (14) is applicable to both fiber tension models: DEM and SDEM. Consequently, the average tensile stress due to steel fibers over the average crack spacing can be calculated by multiplying the result of Eq. (8) or (9) with the coefficient α_{avg} .

In addition to the tensile stress carried by the steel fibers, the tensile stress taken by the concrete matrix should also be taken into account to evaluate the total tensile stress sustained by the SFRC. For this, the following tension softening model⁷ can be employed.

$$f_{ct} = f_{cr} e^{-cw_{cr}} \quad (15)$$

where the coefficient c is 15 and 30 for concrete and mortar, respectively.

Consequently, the tensile stress of SFRC without conventional reinforcements can be evaluated by superposing the contributions of steel fibers and concrete matrix, as follows

$$f_{SFRC} = f_f + f_{ct} \quad (16)$$

Models for SFRC with conventional reinforcement

In SFRC members with conventional reinforcement, the local increase in tensile stress within a reinforcing bar at a crack is transmitted back into the concrete matrix between cracks; this mechanism is commonly referred to as the tension-stiffening effect. Therefore, the average tensile stress of concrete matrix due to the bond mechanism between the concrete matrix and the conventional reinforcement should be evaluated. For the average tensile stress due to the tension stiffening effect, the following model¹⁹ is employed.

$$f_{c,TS} = \frac{f_{cr}}{1 + \sqrt{3.6c_f M \epsilon_{c1}}} \quad (17)$$

where the coefficient c_f considers the effect of steel fibers, evaluated as $c_f = 0.6 + (1/0.034)(l_f/d_f)[(100V_f)^{1.5}/M^{0.8}]$ for end-hooked fibers. The bond parameter M is calculated from $M = A_c/(\sum d_{bs}\pi)$, in millimeters. For reinforced concrete members without steel fibers, the above equation converges to the conventional tension stiffening model^{17,18,24} as c_f becomes 0.6. It is noted that the tensile stress due to the tension stiffening effect should not be less than the tensile stress due to the tension softening effect.^{17,18}

Consequently, the tensile stress in the concrete matrix can be evaluated by considering both the tension-stiffening effect and the stresses transmitted by steel fibers, as follows

$$f_{c1} = f_{c,TS} + (1 - \alpha_{avg}) f_f \cos \theta_f \quad (18)$$

As local yielding of conventional reinforcement at a crack must also be considered, the upper limit of the tensile stress in a concrete matrix can be defined as follows

$$f_{c1} \leq \sum_i \rho_i (f_{scr,i} - f_{s,i}) \cos^2 \theta_{n,i} + (1 - \alpha_{avg}) f_f \cos \theta_f \quad (19)$$

The tensile stresses carried by steel fibers and by tension softening are both calculated for a given crack width, while

the tensile stress due to the tension stiffening effect is calculated for a given average tensile strain. Thus, the average crack spacing is required to establish a relationship between the crack width and the average tensile strain. In this paper, the average crack spacing model recently derived by Deluce et al.²⁵ from the test results with 47 R/FRC members subjected to uniaxial tension has been employed. That is

$$s_{cr} = 2 \left(c_a + \frac{s_b}{10} \right) k_3 + \frac{k_1 k_2}{s_{mi}} \quad (20)$$

where $c = 1.5a_{gg}$; $k_1 = 0.4$; $k_2 = 0.25$; $k_3 = 1 - [\min(V_f, 0.015)/0.015][1 - (1/k_f)]$; a_{gg} is the maximum aggregate size, in millimeters, and

$$s_b = \frac{1}{\sqrt{\sum_i \frac{4 \rho_{s,i}}{\pi d_{b,i}^2} \cos^4 \theta_i}} \quad (21)$$

$$s_{mi} = \sum_i \frac{\rho_{s,i}}{d_{b,i}} \cos^2 \theta_i + k_f \frac{\alpha_f V_f}{d_f} \quad (22)$$

Consequently, the average crack width can be simply evaluated by multiplying the average tensile strain and the average crack spacing $w_{cr} = s_{cr} \epsilon_c$.

In SFRC members containing conventional reinforcement, multiple cracks occur with variable crack widths even under uniformly distributed stress condition. Because the tensile stress transmitted by steel fibers is also influenced by cracks, it is necessary to check whether the tensile stress resisted by steel fibers calculated for the average crack width is not greater than that for the maximum crack width. To consider the maximum crack width, the following model²⁵ has been adopted in this paper.

$$w_{cr,max} = \left(1.7 + 3.4 \frac{V_f I_f}{d_f} \right) w_{cr} \quad (23)$$

Models for shear slip at crack in SFRC with conventional reinforcement

In SFRC panels with conventional reinforcement, the effective direction of the tensile stress taken by steel fibers across a crack may deviate from the principal tensile stress axis within the concrete because of shear slip at a crack, as presented in Fig. 3. Therefore, it is important to consider the effect of steel fibers on the shear slip at a crack. Because shear stress at a crack resisted by fibers bridging a crack has been already subtracted in Eq. (1), by employing the shear stress-slip model for normal reinforced concrete proposed by Vecchio and Lai,²⁶ the shear slip at a crack can be evaluated for the shear stress at the crack calculated from Eq. (1). Therefore, the shear slip at a crack can be calculated accordingly, as follows

$$\delta_s = \delta_2 \sqrt{\frac{\Psi}{1 - \Psi}} \quad (24)$$

$$\delta_2 = \frac{0.5 v_{c,max} + v_{co}}{1.8 w_{cr}^{-0.8} + (0.234 w_{cr}^{-0.707} - 0.20) f_{cc}} \quad (25)$$

where $\Psi = v_{ci,cr}/v_{c,max}$; $v_{c,max} = \sqrt{f'_c} / [0.31 + (24 w_{cr} / a_{gg} + 16)]$, in MPa; $v_{co} = f_{cc}/30$; and f_{cc} is the concrete cube strength, in MPa.

Consequently, the direction of the tensile stress due to steel fibers is deviated by θ_f , which is calculated from the following relationship

$$\theta_f = \tan^{-1} \frac{\delta_s}{w_{cr}} \quad (26)$$

Because θ_f is combined with only the tensile stress due to steel fibers, f_f , all the equations in this paper converge to the equations for normal reinforced concrete members if no steel fibers are provided.

Models for conventional reinforcement

To represent the average tensile stress-strain relationship of conventional reinforcement, a trilinear model can be employed as the following equations

$$f_s = \epsilon_s E_s \text{ for } \epsilon_s \leq \epsilon_{sy} \quad (27)$$

$$f_s = f_{sy} \text{ for } \epsilon_{sy} < \epsilon_s \leq \epsilon_{sh} \quad (28)$$

$$f_s = f_{sy} + (\epsilon_s - \epsilon_{sh}) E_{sh} \text{ for } \epsilon_s > \epsilon_{sh} \quad (29)$$

FINITE ELEMENT IMPLEMENTATION

Once the principal strains are calculated and the appropriate constitutive laws are applied for principal compressive and tensile responses, the analysis of a cracked SFRC panels proceed as for an orthotropic element in the manner described by Vecchio.¹⁸ From the principal stresses and strains, the local material stiffness matrix for concrete can be evaluated by employing secant moduli, as illustrated in Fig. 6.

$$[D_c]' = \begin{bmatrix} \overline{E_{c1}} & 0 & 0 \\ 0 & \overline{E_{c2}} & 0 \\ 0 & 0 & \overline{G_c} \end{bmatrix} \quad (30)$$

where $\overline{E_{c1}} = f_{c1}/\epsilon_{c1}$; $\overline{E_{c2}} = f_{c2}/\epsilon_{c2}$; and $\overline{G_c} = \overline{E_{c1}} \cdot \overline{E_{c2}} / (\overline{E_{c1}} + \overline{E_{c2}})$.

In the same manner as with the concrete matrix, the local material stiffness matrixes for steel fibers and each conventional reinforcement can be defined as follows

$$[D_s]_i' = \begin{bmatrix} \rho_i \overline{E_{si}} & 0 & 0 \\ 0 & 0 & 0 \\ 0 & 0 & 0 \end{bmatrix} \quad (31)$$

for the i -th conventional reinforcement

where $\overline{E_{si}} = f_{s,i}/\epsilon_{s,i}$.

$$[D_f]' = \begin{bmatrix} \overline{E}_{f1} & 0 & 0 \\ 0 & 0 & 0 \\ 0 & 0 & 0 \end{bmatrix} \text{ for steel fibers} \quad (32)$$

where $\overline{E}_{f1} = \alpha_{avg} f_f / \epsilon_{cf}$; and $\epsilon_{cf} = (\epsilon_{c1} + \epsilon_{c2})/2 + [(\epsilon_{c1} - \epsilon_{c2})/2] \times \cos 2\theta_f$.

After transforming the local material stiffness matrices to the global axis, the global stiffness matrix for a SFRC panel is obtained as follows

$$[D] = [D_c] + [D_f] + \sum_7 [D_{s,i}] \quad (33)$$

where $[D_c] = [T_c]^T [D_c] [T_c]$; $[D_f] = [T_f]^T [D_f] [T_f]$; $[D_{s,i}] = [T_{s,i}]^T [D_{s,i}] [T_{s,i}]$; and

$$[T] = \begin{bmatrix} \cos^2 \psi & \sin^2 \psi & \cos \psi \sin \psi \\ \sin^2 \psi & \cos^2 \psi & -\cos \psi \sin \psi \\ -2 \cos \psi \sin \psi & 2 \cos \psi \sin \psi & (\cos^2 \psi - \sin^2 \psi) \end{bmatrix} \quad (34)$$

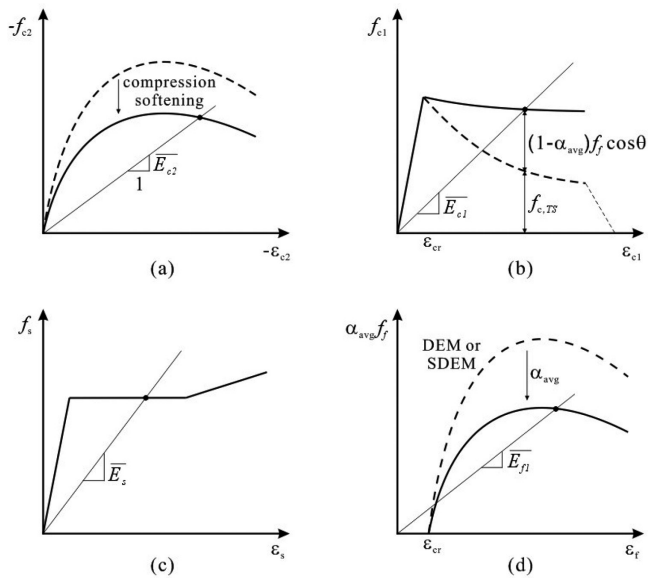


Fig. 6—Constitutive relations and secant moduli: (a) concrete matrix under compression; (b) concrete matrix under tension; (c) conventional reinforcements; and (d) steel fibers.

Table 1—Concrete and steel fiber material properties of SFRC panels¹⁴

Specimens	Concrete		Steel fibers		
	f'_c , MPa (ksi)	l_f , mm (in.)	d_f , mm (in.)	σ_{fu} , mm (in.)	V_f , %
C1F1V1	51.4 (7.45)	50.0 (1.97)	0.62 (0.024)	1050 (152)	0.5
C1F1V2	53.4 (7.75)	50.0 (1.97)	0.62 (0.024)	1050 (152)	1.0
C1F1V3	49.7 (7.21)	50.0 (1.97)	0.62 (0.024)	1050 (152)	1.5
C1F2V3	59.7 (8.66)	30.0 (1.18)	0.38 (0.015)	2300 (334)	1.5
C1F3V3	45.5 (6.60)	35.0 (1.38)	0.55 (0.022)	1100 (160)	1.5
C2F1V3	78.8 (11.43)	50.0 (1.97)	0.62 (0.024)	1050 (152)	1.5
C2F2V3	76.5 (11.10)	30.0 (1.18)	0.38 (0.015)	2300 (334)	1.5
C2F3V3	62.0 (8.99)	35.0 (1.38)	0.55 (0.022)	1100 (160)	1.5

where $\psi = \theta_c$ for the concrete (that is, inclination of the net principal tensile stress); $\psi = \theta_c + \theta_f$ for steel fibers (that is, inclination of the tensile stress due to steel fibers; refer to Fig. 3); and $\psi = \alpha_i$ for i -th conventional reinforcement (that is, orientation of reinforcing bar).

With the global stiffness matrix for a SFRC element established, the relationship between the stresses induced by external load and the total strains can be expressed as follows

$$[\sigma] = [D][\epsilon] - [\sigma^0] \quad (35)$$

where $[\sigma] = [\sigma_x \ \sigma_y \ \tau_{xy}]^T$, $[\epsilon] = [\epsilon_x \ \epsilon_y \ \gamma_{xy}]^T$, and $[\sigma^0] = [D_c][\epsilon^s]$.

COMPARISON WITH SFRC PANEL TEST RESULTS

Test panel details

For verification of the proposed analysis procedure, eight SFRC panels tested by Susetyo et al.¹⁴ were analyzed. The test variables, summarized in Table 1, were concrete compressive strength (with target strengths of 50 and 80 MPa [7.25 and 11.60 ksi] for C1 and C2, respectively), fiber volumetric ratio (0.5, 1.0, and 1.5% for V1, V2, and V3, respectively), and fiber type (end-hooked fibers: F1, F2, and F3). The SFRC panels were 890 x 890 mm square and 70 mm thick (35 x 35 x 2.75 in.), and contained longitudinal steel reinforcement in the ratio of 3.31% with a yield strength of 552.2 MPa (80.1 ksi); no transverse reinforcement was provided. The panels were loaded in a pure shear stress condition, using a monotonically increasing force-controlled protocol, until the panels failed. Material properties for concrete and steel fibers are given in Table 1. Details of the SFRC panels and a representative failure mode are presented in Fig. 7.

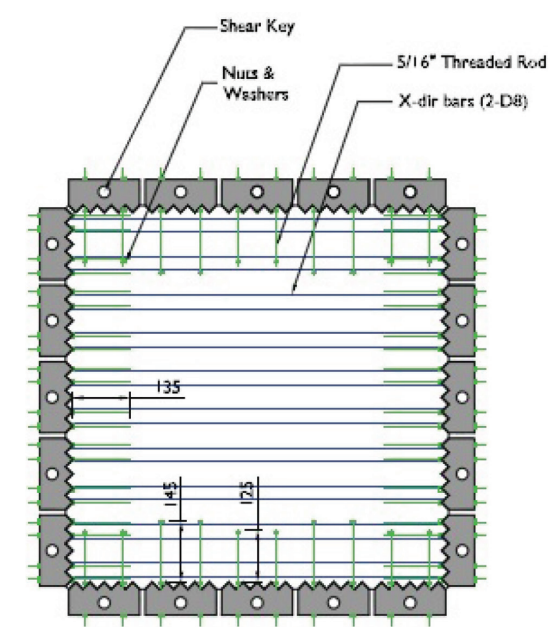
Comparison of analysis results and test results

In Table 2 and Fig. 8, the shear strengths and strains at failure predicted by the proposed analysis procedure are presented and compared with the test results. As evident in the table and figures, the analysis results are in good agreement with the tests; for the eight specimens, the ratio of the calculated shear strength to measured shear strength had a mean of 0.99 and a coefficient of variation (CoV) of 0.11; for the shear strains at peak stress, the ratio had a mean of 0.99 and a CoV of 0.24.

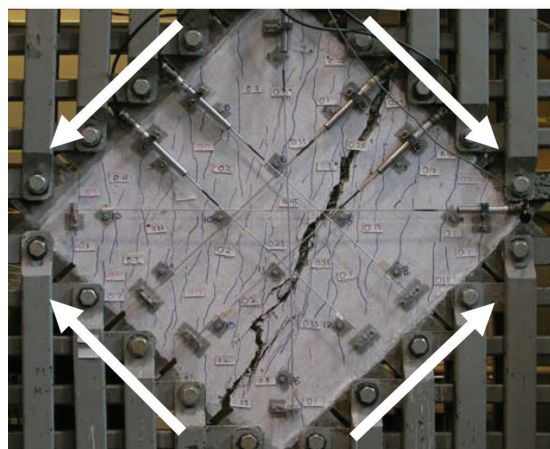
Figures 9 and 10 provide comparisons of the calculated and experimentally observed responses for all panel spec-

Table 2—Comparison of analysis and test results for SFRC shear panels

Specimen	Analysis		Test		Analysis/Test	
	$\tau_{xy,u}$, MPa (ksi)	$\gamma_{xy,u} \times 10^{-3}$	$\tau_{xy,u}$, MPa (ksi)	$\gamma_{xy,u} \times 10^{-3}$	$\frac{\tau_{xy,u,Analysis}}{\tau_{xy,u,Test}}$	$\frac{\gamma_{xy,u,Analysis}}{\gamma_{xy,u,Test}}$
C1F1V1	3.21 (0.466)	4.03	3.53 (0.512)	2.77	0.91	1.46
C1F1V2	5.13 (0.744)	5.49	5.17 (0.750)	5.27	0.99	1.04
C1F1V3	6.68 (0.968)	5.40	5.37 (0.779)	5.10	1.24	1.06
C1F2V3	6.15 (0.892)	5.81	6.68 (0.969)	6.35	0.92	0.91
C1F3V3	4.75 (0.689)	4.06	5.59 (0.811)	4.27	0.85	0.95
C2F1V3	6.61 (0.959)	2.95	6.90 (1.001)	5.25	0.96	0.56
C2F2V3	6.81 (0.987)	4.83	6.31 (0.915)	4.35	1.08	1.11
C2F3V3	5.46 (0.791)	4.20	5.57 (0.808)	4.97	0.98	0.85
			Average		0.99	0.99
			CoV		0.11	0.24

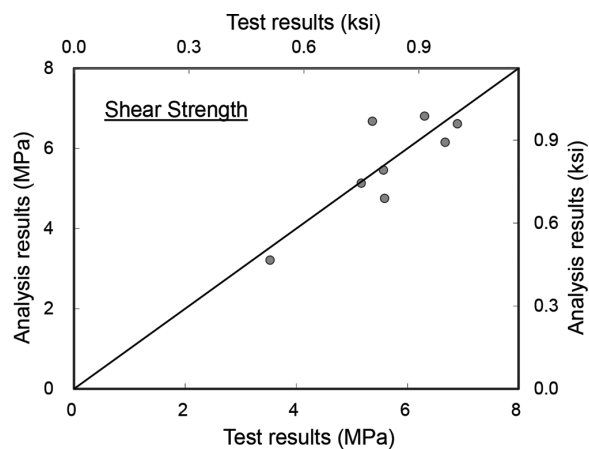


(a)

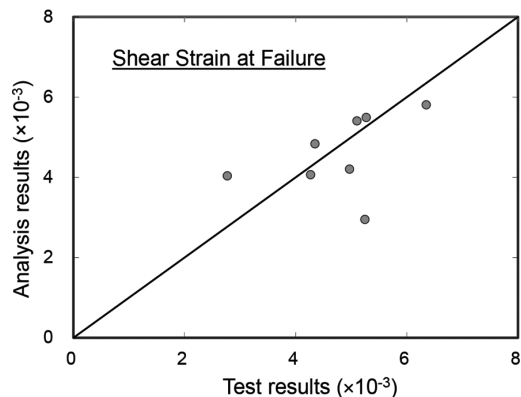


(b)

Fig. 7—Details of SFRC panels: (a) reinforcement configuration; and (b) failure mode of C1F1V3.



(a)



(b)

Fig. 8—Comparison of test and analysis results for shear strength and shear strain at failure: (a) shear strength; and (b) shear strain at failure.

imens. As seen in Fig. 9, the shear stress-strain responses of the SFRC panels were predicted well by the proposed analysis procedure. The minor deviations observed are mainly due to variances in the predictions of the SFRC tension model (that is, DEM), as revealed in Fig. 10. The

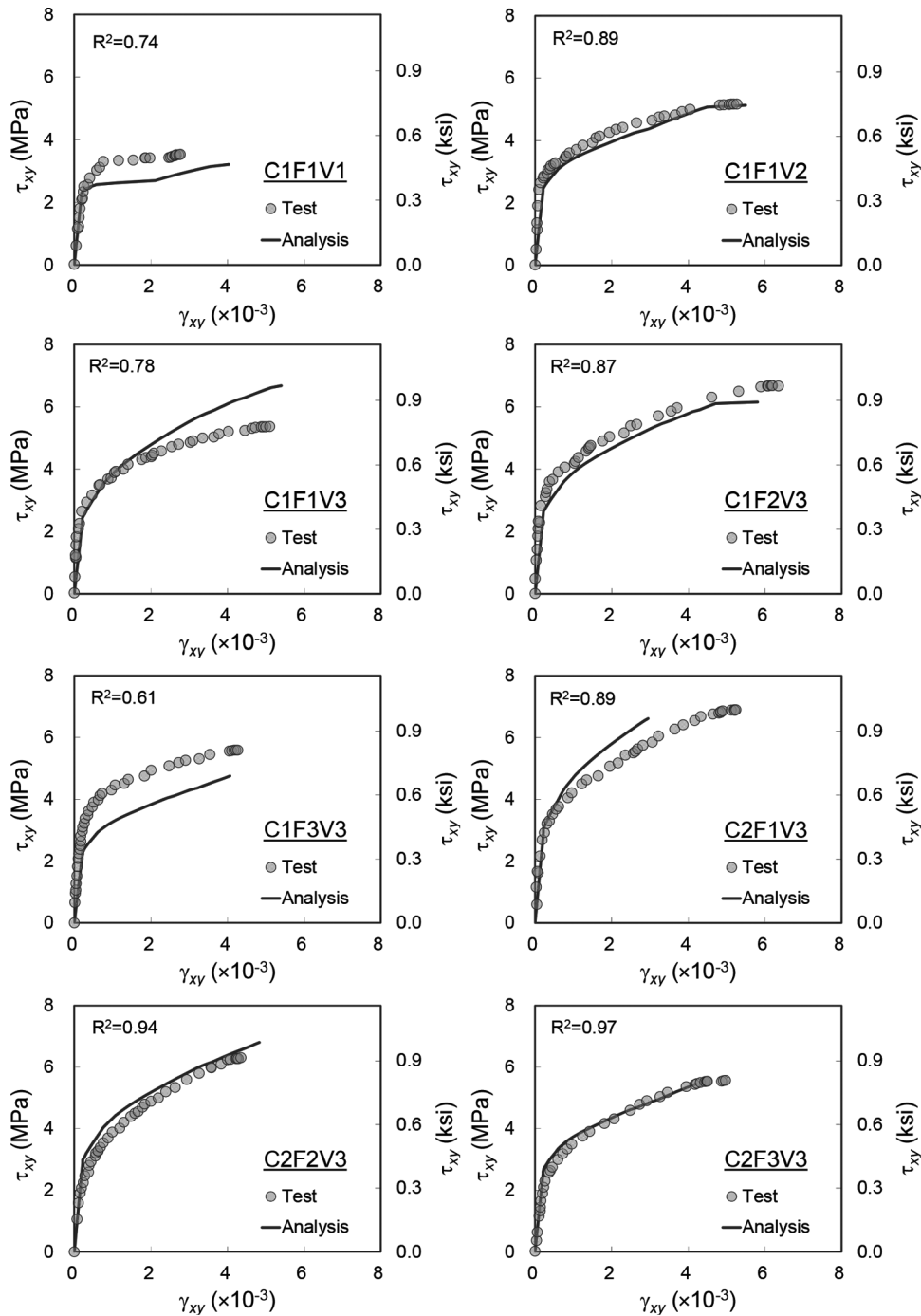


Fig. 9—Comparison of test and analysis results for shear stress-strain response.

total tensile stress in SFRC (that is, the sum of tensile stresses due to steel fibers and concrete matrix) was overestimated for C1F1V3, whereas it was underestimated for C1F3V3. The shear at failure for C2F1V3 was underestimated because of rupture of the steel fibers, which is more difficult to capture analytically. Panel C1F1V1 exhibited a relatively brittle behavior after cracking because of its low fiber volumetric ratio; for this panel, there is some difference in the peak strain response, although the predicted strength accurately matches with the test result. Panel C1F3V3 was overestimated because it exhibited principal tensile stress higher than C2F3V3; for this panel, some test anomalies may have occurred. Overall, from Fig. 9 and 10, it can be

inferred that any discrepancy in the shear behavior of SFRC panels between the predictions and the test results is mainly due to error in the evaluation of tensile stress provided by steel fibers, and is not symptomatic of the developed analysis procedure. In spite of these discrepancies, the predictions for the shear behavior of SFRC panels are generally within an acceptable range. In general, the shear stress-strain response were well predicted when the uniaxial tensile behavior of SFRC was well predicted. Consequently, it can be concluded that the actual structural behavior of SFRC panels subjected to pure shear is well predicted by the proposed analysis procedure, not only for the shear stress-strain response but also principal tensile stress-strain response in the panels.

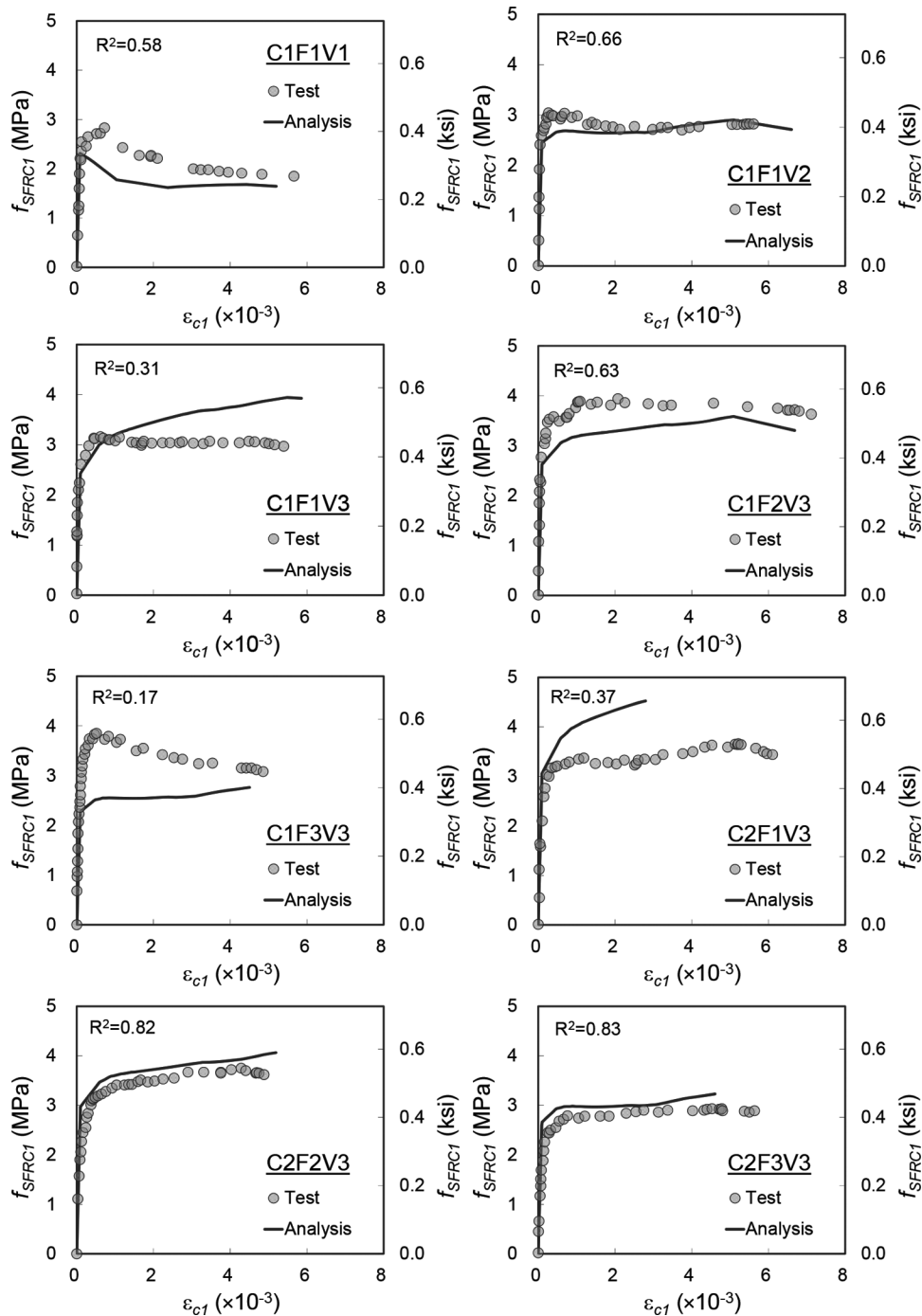


Fig. 10—Comparison of test and analysis results for SFRC principal tensile stress-strain response.

CONCLUSIONS

In this paper, an advanced analysis procedure has been developed for modeling the shear behavior of SFRC elements. Different from the approach generally adopted in previous works in the literature, where the tensile stress of concrete was simply increased to consider the contribution of steel fibers, the contributions of the three materials—concrete matrix, conventional reinforcement, and steel fibers—were considered separately in the proposed analysis procedure. For the evaluation of the stresses due to steel fibers, the constitutive models for the tensile behavior of SFRC (DEM and SDEM) and cracking behavior models for SFRC members with conventional reinforcement (tension

stiffening model and crack spacing model) were employed so that the contribution of steel fibers was rigorously taken into the account.

The proposed analysis procedure was verified through comparisons with the test results of SFRC panels. With the proposed analysis procedure, not only the shear strength but also the shear strain at failure were predicted sufficiently well. In addition, it was shown that the proposed analysis procedure captures well the principal tensile stress-strain response of SFRC, which is a dominant behavior in SFRC panels with conventional reinforcement.

Consequently, it is concluded that the actual shear behavior of SFRC panels can be modeled reasonably accurately by

the proposed analysis procedure. Because it can be easily implemented in sectional analysis programs or finite element analysis programs that are based on a smeared rotating crack approach, the proposed analysis procedure will be useful for predictions of the actual SFRC members or structures with conventional reinforcement.

AUTHOR BIOS

ACI member **Seong-Cheol Lee** is an Associate Professor at KEPCO International Nuclear Graduate School (KINGS), South Korea. He received his PhD from Seoul National University, Seoul, Korea, in 2007, and was then a postdoctoral researcher in the Department of Civil Engineering at the University of Toronto, Toronto, ON, Canada. His research interests include the shear behavior of concrete structures and the analysis of prestressed concrete structures and fiber-reinforced concrete members.

ACI member **Jae-Yeol Cho** is an Associate Professor in the Department of Civil & Environmental Engineering at Seoul National University, where he received his PhD. His research interests include nonlinear analysis and optimized design of reinforced and prestressed concrete structures, material modeling, and similitude laws for dynamic test of concrete structures.

Frank J. Vecchio, F.ACI, is a Professor in the Department of Civil Engineering at the University of Toronto. He is a member of Joint ACI-ASCE Committees 441, Reinforced Concrete Columns, and 447, Finite Element Analysis of Reinforced Concrete Structures. His research interests include nonlinear analysis and design of reinforced concrete structures, constitutive modeling, performance assessment and forensic investigation, and repair and rehabilitation of structures.

ACKNOWLEDGMENTS

This research was supported by the Korea Institute of Energy Technology Evaluation and Planning (KETEP), funded by the Ministry of Knowledge Economy (No. 2011T100200162), supported by the Nuclear Safety Research Program through the Korea Foundation of Nuclear Safety (KOFONS) granted financial resource from the Nuclear Safety and Security Commission (NSSC) (No. 1305009), and supported by the Institute of Construction and Environmental Engineering at Seoul National University. Support was also provided by the Natural Sciences and Engineering Research Council of Canada (NSERC).

NOTATION

$[D]$	= element stiffness matrix for SFRC with conventional reinforcement
$[D_c]'$	= material stiffness matrix for concrete
$[D_f]'$	= material stiffness matrix for steel fibers
$[D_s]_i'$	= material stiffness matrix for i -th conventional reinforcement
d_{bs}	= diameter of conventional reinforcement
d_f	= fiber diameter
E_c	= elastic modulus of concrete
E_s	= elastic modulus of conventional reinforcement
E_{sh}	= strain hardening modulus of conventional reinforcement
f_c'	= compressive strength of concrete cylinder
$f_{c,TS}$	= average tensile stress in concrete due to tension stiffening effect
f_{c1}	= principal tensile stress in concrete
f_{c2}	= principal compressive stress in concrete
$f_{c,max}$	= peak compressive stress in concrete considering compression softening effect
f_{cr}	= cracking strength of concrete
f_{ct}	= tensile stress in concrete due to tension softening effect
f_{eh}	= tensile stress due to mechanical anchorage effect of end-hooked steel fibers
f_f	= tensile stress at crack due to steel fibers
f_{SFRC}	= tensile stress of SFRC
f_s	= average stress in conventional reinforcement
f_{scr}	= local stress (at crack) in conventional reinforcement
f_{st}	= tensile stress due to frictional bond behavior of steel fibers
f_{sy}	= yield strength of conventional reinforcement
l_f	= fiber length
l_i	= distance between mechanical anchorages for end-hooked fiber
s_{cr}	= average crack spacing in principal tensile stress direction in concrete
s_{eh}	= slip at maximum tensile force due to mechanical anchorage of fiber with inclination angle of 0 degrees to normal of crack surface

s_f	= slip at frictional bond strength for fiber with inclination angle of 0 degrees
$[T]$	= rotation transformation matrix
V_f	= fiber volumetric ratio
$v_{ci,cr}$	= shear stress on crack surface
w_{cr}	= average crack width
$w_{cr,max}$	= maximum crack width
α_{avg}	= coefficient to relate tensile stress at a crack due to steel fibers with average tensile stress
α_f	= fiber orientation factor
β_{fs}, β_{eh}	= coefficients to consider effect of fiber slip on longer embedment side on frictional behavior and mechanical anchorage effect, respectively
δ_s	= slip displacement along crack surface
$[\epsilon]$	= apparent (total) average strains in elements including crack slip strains
$[\epsilon_c]$	= average strains in concrete
ϵ_c'	= strain at concrete compressive strength
ϵ_{c1}	= average strain in concrete in principal tensile stress direction
ϵ_{c2}	= average strain in concrete in principal compressive stress direction
$[\epsilon^*]$	= equivalent average strains due to discontinuous slip along crack
ϵ_{sh}	= hardening strain of conventional reinforcement
ϵ_{sy}	= yield strain of conventional reinforcement
γ_s	= shear strain due to slip along crack surface
θ_c	= inclination of principal tensile stress in concrete
θ_f	= angle between tensile stress direction due to steel fibers and principal tensile stress direction in concrete
θ_n	= angle between conventional reinforcement and normal to crack
ρ_s	= reinforcement ratio
$[\sigma]$	= total stress of SFRC elements with conventional reinforcement
$[\sigma^0]$	= offset stress due to crack slip
$\sigma_{f,cr,avg}$	= average fiber tensile stress at crack
$\sigma_{f,cr}(l_a, \theta)$	= fiber tensile stress at crack for given shorter embedment length l_a and fiber inclination angle θ
$\tau_{eh,max}$	= equivalent bond strength due to mechanical anchorage of steel fiber
$\tau_{f,max}$	= frictional bond strength of steel fiber

REFERENCES

- Petersson, P. E., "Fracture Mechanical Calculations and Tests for Fiber-Reinforced Cementitious Materials," *Proceedings of Advances in Cement-Matrix Composites*, Materials Research Society, Boston, MA, 1980, pp. 95-106.
- Li, Z.; Li, F.; Chang, T.-Y. P.; and Mai, Y.-W., "Uniaxial Tensile Behavior of Concrete Reinforced with Randomly Distributed Short Fibers," *ACI Materials Journal*, V. 95, No. 5, Sept.-Oct. 1998, pp. 564-574.
- Groth, P., "Fibre Reinforced Concrete—Fracture Mechanics Methods Applied on Self-Compacting Concrete and Energetically Modified Binders," doctorate thesis, Luleå University of Technology, Department of Civil and Mining Engineering, Division of Structural Engineering, Luleå, Sweden, 2000, 237 pp.
- Barragán, B. E.; Gettu, R.; Martín, M. A.; and Zerbino, R. L., "Uniaxial Tension Test for Steel Fibre Reinforced Concrete—A Parametric Study," *Cement and Concrete Composites*, V. 25, No. 7, 2003, pp. 767-777. doi: 10.1016/S0958-9465(02)00096-3
- Lim, T. Y.; Paramasivam, P.; and Lee, S. L., "Analytical Model for Tensile Behavior of Steel-Fiber Concrete," *ACI Materials Journal*, V. 84, No. 4, July-Aug. 1987, pp. 286-298.
- Marti, P.; Pfyf, T.; Sigrist, V.; and Ulaga, T., "Harmonized Test Procedures for Steel Fiber-Reinforced Concrete," *ACI Materials Journal*, V. 96, No. 6, Nov.-Dec. 1999, pp. 676-686.
- Voo, J. Y. L., and Foster, S. J., "Variable Engagement Model for Fibre Reinforced Concrete in Tension," *Uniciv Report No. R-420*, University of New South Wales, School of Civil and Environmental Engineering, June 2003, 86 pp.
- Lee, S.-C.; Cho, J.-Y.; and Vecchio, F. J., "Diverse Embedment Model for Fiber-Reinforced Concrete in Tension: Model Development," *ACI Materials Journal*, V. 108, No. 5, Sept.-Oct. 2011, pp. 516-525.
- Lee, S.-C.; Cho, J.-Y.; and Vecchio, F. J., "Diverse Embedment Model for Fiber-Reinforced Concrete in Tension: Model Verification," *ACI Materials Journal*, V. 108, No. 5, Sept.-Oct. 2011, pp. 526-535.
- Lee, S.-C.; Cho, J.-Y.; and Vecchio, F. J., "Simplified Diverse Embedment Model for Steel Fiber-Reinforced Concrete Elements in Tension," *ACI Materials Journal*, V. 110, No. 4, July-Aug. 2013, pp. 403-412.

11. CEB-FIP, "CEB-FIP Model Code 2010 Final Draft." Comité Euro-International du Béton, Lausanne, Switzerland, 2011, 653 pp.
12. BS EN 14651, "Test Method for Metallic Fibre Concrete – Measuring the Flexural Tensile Strength (Limit of Proportionality (LOP), Residual," British Standards Institution, London, UK, 2007, pp. 1-20.
13. Dinh, H. H.; Parra-Montesinos, G. J.; and Wight, J. K., "Shear Behavior of Steel Fiber-Reinforced Beams without Stirrup Reinforcement," *ACI Structural Journal*, V. 107, No. 5, Sept.-Oct. 2010, pp. 597-606.
14. Susetyo, J.; Gauvreau, P.; and Vecchio, F. J., "Effectiveness of Steel Fiber as Minimum Shear Reinforcement," *ACI Structural Journal*, V. 108, No. 4, July-Aug. 2011, pp. 488-496.
15. ACI Committee 318, "Building Code Requirements for Structural Concrete (ACI 318-11) and Commentary," American Concrete Institute, Farmington Hills, MI, 2011, 503 pp.
16. Susetyo, J.; Gauvreau, P.; and Vecchio, F. J., "Steel Fiber-Reinforced Concrete Panels in Shear: Analysis and Modeling," *ACI Structural Journal*, V. 110, No. 2, Mar.-Apr. 2013, pp. 285-295.
17. Vecchio, F. J., "Disturbed Stress Field Model for Reinforced Concrete: Formulation," *Journal of Structural Engineering*, ASCE, V. 126, No. 9, 2000, pp. 1070-1077. doi: 10.1061/(ASCE)0733-9445(2000)126:9(1070)
18. Vecchio, F. J., "Disturbed Stress Field Model for Reinforced Concrete: Implementation," *Journal of Structural Engineering*, ASCE, V. 127, No. 1, 2001, pp. 12-20. doi: 10.1061/(ASCE)0733-9445(2001)127:1(12)
19. Lee, S.-C.; Cho, J.-Y.; and Vecchio, F. J., "Tension-Stiffening Model for Steel Fiber-Reinforced Concrete Containing Conventional Reinforcement," *ACI Structural Journal*, V. 110, No. 4, July-Aug. 2013, pp. 639-648.
20. Bentz, E. C., "Sectional Analysis of Reinforced Concrete Members," doctorate thesis, Department of Civil Engineering, University of Toronto, Toronto, ON, Canada, 2000, 184 pp.
21. Wong, P. S.; Vecchio, F. J.; and Trommels, H., "VecTor2 & FormWorks User's Manual, second edition," University of Toronto, Department of Civil Engineering, Toronto, ON, Canada, Aug. 2013, 318 pp.
22. Vecchio, F. J., and Collins, M. P., "The Modified Compression Field Theory for Reinforced Concrete Elements Subjected to Shear," *ACI Journal Proceedings*, V. 83, No. 2, Mar.-Apr. 1986, pp. 219-231.
23. Lee, S.-C.; Oh, J.-H.; and Cho, J.-Y., "Compressive Behavior of Fiber-Reinforced Concrete with End-Hooked Steel Fibers," *Materials*, V. 8, 2015, pp. 1442-1458. doi: 10.3390/ma8041442
24. Bentz, E. C., "Explaining the Riddle of Tension Stiffening Models for Shear Panel Experiments," *Journal of Structural Engineering*, ASCE, V. 131, No. 9, 2005, pp. 1422-1425. doi: 10.1061/(ASCE)0733-9445(2005)131:9(1422)
25. Deluce, J. R.; Lee, S.-C.; and Vecchio, F. J., "Crack Model for Steel Fiber-Reinforced Concrete Members Containing Conventional Reinforcement," *ACI Structural Journal*, V. 111, No. 1, Jan.-Feb. 2014, pp. 93-102.
26. Vecchio, F. J., and Lai, D., "Crack Shear-Slip in Reinforced Concrete Elements," *Journal of Advanced Concrete Technology*, V. 2, No. 3, 2004, pp. 289-300. doi: 10.3151/jact.2.289

Reproduced with permission of the copyright owner. Further reproduction prohibited without permission.